

Cubic phases of BC₂N: A first-principles study

Eunja Kim* and Tao Pang

Department of Physics and Astronomy, University of Nevada, Las Vegas, Nevada 89154, USA

Wataru Utsumi

Synchrotron Radiation Research Center, Japan Atomic Energy Research Institute, Kashiwa-shi, Chiba-ken 277-0842, Japan

Vladimir L. Solozhenko

LPMTM-CNRS, Universite Paris Nord, 93430 Villetaneuse, France

Yusheng Zhao

Los Alamos National Laboratory, Los Alamos, New Mexico 87545, USA

(Received 16 February 2007; published 30 May 2007)

First-principles calculations are performed and analyzed to identify different cubic phases of BC₂N synthesized experimentally. With a proper choice of the supercell, cutoff energy, and sampling k points, the cubic phases are found to be stable theoretically. The bulk modulus from elastic stiffness constants for each of the phases is in excellent agreement with available experimental data. All the phases are defect-free and do not possess any B–B or N–N bond. Two high-density phases with nearly degenerate energies are interpreted to represent two experimental systems of different x-ray patterns. The high-density phases are characterized by the existence of C–C bonds, whereas the low-density phase is characterized by the absence of C–C bonds. From the calculated equation of state and the available experimental data, we show that the unique feature of each of the cubic BC₂N phases is a direct result of the corresponding local electronic structure and chemical bonding in the system.

DOI: [10.1103/PhysRevB.75.184115](https://doi.org/10.1103/PhysRevB.75.184115)

PACS number(s): 64.30.+t, 71.15.Nc, 81.40.Vw, 64.10.+h

The quest for a material with its hardness over that of diamond has been pursued actively in recent years.¹ While diamond remains to be the material of choice in cutting and polishing metals and other hard solids, its superiority runs into resistance in cutting certain tough materials such as ferrous metals.² Synthetic materials with a comparable hardness, such as cubic boron nitride (c -BN), are potential candidates to palliate this limitation. Various c -BN structures have been studied extensively both experimentally^{3–11} and theoretically.^{12–19} The closely related BC₂N ternaries have also been synthesized and characterized by several groups using high-pressure and high-temperature techniques;^{20–26} it is found that different experimental conditions, such as temperature, pressure, or starting material, can render a different final structure. A detailed study of the interplay between temperature and pressure during experimental processes has been carried out by Nakano *et al.*²² with various starting materials.

High-density cubic (c -) BC₂N structures have been synthesized by Utsumi *et al.*²⁴ and Zhao *et al.*,²⁵ and the reported lattice parameters in both cases obey Vegard's law for solid solutions. A convergent picture of these experimentally found structures has emerged after many theoretical efforts, as exemplified by the work of Sun *et al.*¹⁵

With different pressure (18 GPa), temperature (2200 K), and starting material (graphitic BC₂N), Solozhenko *et al.*²⁶ have obtained a quite different cubic structure that has a much lower density. The lattice constant and bulk modulus of this low-density c -BC₂N are found to be about 3.642 Å and 282 GPa, respectively, in contrast to those of the high-density structures of about 3.60 Å and 345 GPa,^{24,25} respectively. In spite of many experimental and theoretical efforts,

the underlying mechanism that leads to the property difference between the high-density and low-density c -BC₂N structures is still unclear; the gap between calculations and experimental measurements of the bulk modulus for each of c -BC₂N phases remains.

Our goal here is threefold. First, we want to perform the most accurate first-principles calculations of the electronic structure for each of the c -BC₂N phases, including chemical bonding, lattice constant, and bulk modulus. Then we want to provide an explanation to the distinctive features between the high-density phases and the low-density phase found experimentally, especially the subtle difference in the two competing high-density phases shown in the x-ray patterns. This also includes attributing the absence of any C–C bond as the cause of the enlarged lattice constant and lowered bulk modulus in the low-density phase. Then we make a detailed comparison between the calculated equation of state and the available experimental measurements. Based on this comparative study, we propose the corresponding structure for each of the phases.

The standard density-functional theory²⁷ is used in carrying out all the calculations presented here. The generalized gradient approximation of Perdew *et al.*²⁸ is adopted in the construction of the exchange and correlation interaction. The Troullier-Martins²⁹ pseudopotentials of carbon, boron, and nitrogen are used in the calculations. Convergence tests for the pseudopotentials are carried out on diamond (c -C), c -BN, and c -BC₂N in order to find a suitable choice of k points and plane waves. For all the calculations reported here, we have used a cutoff energy of 110 Ry, which results in an energy convergence on the order of about 10^{−4} eV. A

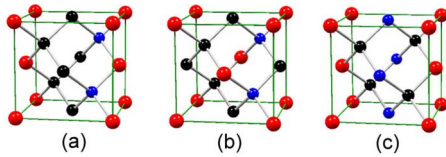


FIG. 1. (Color online) The cubic BC_2N structures that we have found to describe the relevant phases obtained experimentally: (a) The high-density phase (HD1) with C-B-N layered superstructure, (b) the high-density phase (HD2) without any C-B-N layers, and (c) the low-density (LD) phase without any C-C bond. Black, red, and blue symbols are for carbon, boron, and nitrogen, respectively.

total of 64 atoms are included in each of the supercells. These choices ensure accurate lattice constants for c - BC_2N . The k points are sampled in the Brillouin zone under the Monkhorst-Pack³⁰ grid of $2 \times 2 \times 2$.

In Fig. 1 we show the most plausible theoretical structures that we have found for c - BC_2N at high density and low density based on the first-principles calculations. All these structures are defect-free and stable cubic lattices with possible deviations in lattice constants b and c less than 1% from lattice constant a , and do not possess any B-B or N-N bond. The structure given in Fig. 1(a) has widely been accepted as the high-density structure (HD1) for the high-density phase of c - BC_2N and contains only C-C, B-N, C-N, and C-B chemical bonds.¹⁵ Later we will argue that HD1 is the proper structure for the high-density phase synthesized by Utsumi *et al.*²⁴ The structure shown in Fig. 1(b) is another plausible high-density structure (HD2) that is energetically nearly degenerate with HD1 because of the similarity in bonding characteristics, namely, with all the C-C, B-N, C-N, and C-B bonds. Later we will argue that HD2 is the proper structure for the high-density phase synthesized by Zhao *et al.*²⁵ The structure shown in Fig. 1(c) is our proposed low-density (LD) structure for the low-density phase synthesized by Solozhenko *et al.*²⁶ Structure LD does not have any C-C, B-B, or N-N bond.

The lattice constant, cohesive energy, and bulk modulus of each of the three structures shown in Fig. 1 are summarized in Table I. We have also listed experimental data from Utsumi *et al.*²⁴ and Zhao *et al.*²⁵ and theoretical calculations of Sun *et al.*¹⁵ The lattice constant for each of the three structures from Sun *et al.*¹⁵ is an average of the three sides of the unit cell due to the orthorhombic distortion in the stable structure found there. Our calculation of the lattice constants are in excellent agreement with the experimental values and consistent with the calculations of Sun *et al.* The calculated structural properties such as lattice constants, cohesive energies, and bulk moduli for the two high-density phases (HD1 and HD2) are very close because of the similarity in their chemical bonding characteristics. However, a close examination of the atomic arrangements in the two structures tells that HD1 contains an embedded superstructure made of carbon and boron-nitride layers. Later we will argue that this is the source of the weak (200) line in the x-ray pattern of the lattice. HD1 and HD2 are more favorable energetically than any other stable cubic structure of BC_2N at a similar density.

The lattice constant for the (LD) phase is found in

TABLE I. The calculated lattice constant a (Å), cohesive energy E_c (eV), bulk modulus B_0 (GPa), and elastic stiffness constants C_{ij} (GPa) of c - BC_2N are given for each of the three structures (HD1, HD2, and LD) shown in Fig. 1. Available experimental data (given in parentheses) and previous theoretical calculations of Sun *et al.* are all shown for comparison.

	HD1	HD2	LD
a	3.61 (3.595) ^a 3.583 ^d	3.61 (3.595) ^b 3.582 ^d	3.64 (3.642) ^c 3.601 ^d
E_c	7.977	7.974	7.536
B_0	342.4 (345) ^a 399.7 ^d	344.7 400.1 ^d	289.6 (282) ^c 369.9 ^d
C_{44}	453.6 484.2 ^d	458.5 493.0 ^d	391.0 456.3 ^d
$(C_{11}-C_{12})/2$	374.8 352.4 ^d	389.2 314.3 ^d	375.8 366.3 ^d

^aReference 24.

^bReference 25.

^cReference 26.

^dReference 15.

excellent agreement with experiments. The cohesive energy of each atom in LD is about 5% less than the corresponding value in HD1 or HD2. Not only have we found a stable cubic structure for the low-density phase, but the lattice constant obtained here also shows an improvement over the corresponding theoretical value obtained previously.¹⁵

The bulk modulus for each structure is extracted from the elastic stiffness constants. Because we are working on cubic lattices, the bulk modulus is given by $B_0 = (C_{11} + 2C_{12})/3$, where C_{ij} are elastic stiffness constants of the lattice.³¹ Previous density-functional calculations of the bulk modulus^{15,32} are about 16% higher than the corresponding experimental value. This discrepancy usually comes from the wrong assumption of a quadratic energy-volume curve or the Murnaghan equation of state.³³ However, the energy-volume curve for any c - BC_2N phase is quadratic only if it is very close to the minimum-energy point. The nonquadratic contributions can amount up to 20%.³⁴ This is the reason for us to calculate the bulk modulus from the elastic stiffness constants. The bulk modulus is slightly higher (about 9%) if the local-density approximation is used instead of the generalized gradient approximation. For all the structures considered, the calculated bulk moduli are in excellent agreement with the available experimental data. No experimental measurement on bulk modulus is available for HD2, but the actual value should be very close to that of HD1 based on their similarity in the chemical bonding characteristics. As shown in Fig. 1(c), no chemical bond is found between any identical elements. This is the reason for a lower cohesive energy, an enlarged lattice constant, and a lowered bulk modulus in the low-density phase.

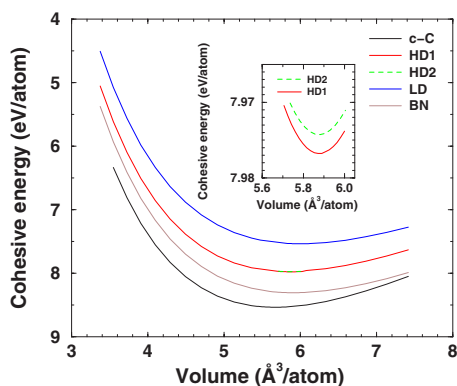


FIG. 2. (Color online) Cohesive energy curves for the three structures (HD1, HD2, and LD) shown in Fig. 1. The corresponding curves of diamond ($c\text{-C}$) and $c\text{-BN}$ are also shown for comparison. The difference between HD1 and HD2 structures is enlarged in the inset.

In Fig. 2, we show the calculated cohesive energy curves of the three structures given in Fig. 1. Our calculations reveal that C–C bonds in the high-density phases cause higher cohesive energies and bulk moduli than those in the low-density phase. From the relation between the three cohesive energy curves of HD1, HD2, and LD for formula $c\text{-BC}_2\text{N}$ and those of diamond and $c\text{-BN}$, we can certainly see the trend: The greater the resemblance to diamond and $c\text{-BN}$ in the local structure, the higher the cohesive energy, the shorter the lattice constant, and larger the bulk modulus. This is implied from Vegard’s law; for example, the cohesive energy, lattice constant, and bulk modulus of an ideally mixed diamond and $c\text{-BN}$ (the superlayered BC_2N) are right between those of diamond and $c\text{-BN}$. All the other BC_2N structures are then expected to be ternaries (HD1, HD2, and LD shown in Fig. 1, for example) and have smaller cohesive energies, larger lattice constants, and lower bulk moduli. All the BC_2N phases can also be studied at ambient pressure, as is given elsewhere.^{18,35}

In Fig. 3, we show the calculated volume compression compared with available experimental data. The volume-pressure relations found for the high-density phases (HD1 and HD2) are in excellent agreement with the experimental measurement of Utsumi *et al.*²⁴ The volume-pressure relation found for the (LD) phase is also in excellent agreement with the experimental measurement of Solozhenko *et al.*²⁶ This nearly perfect agreement between theory and experiment is remarkable because no adjustable parameters are ever introduced in our calculations. It is the strongest support to our proposed structural descriptions of the high-density phases and low-density phase shown in Fig. 1. One issue still remains though in distinguishing the two seemingly similar high-density structures. Our calculations provide quantitative descriptions of the different phases of formula $c\text{-BC}_2\text{N}$. Furthermore, we have obtained a clear picture on the long-sought description of the low-density phase of $c\text{-BC}_2\text{N}$ synthesized by Solozhenko *et al.*;²⁶ the absence of C–C bonds is the most fundamental physics involved in the phase.

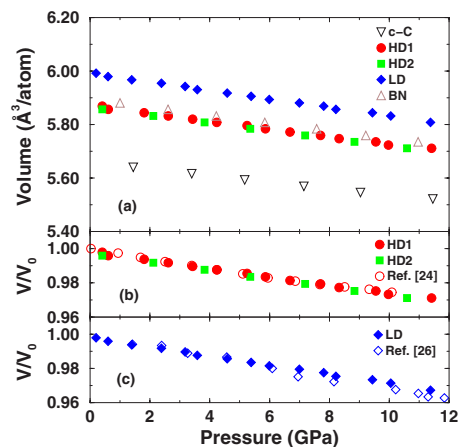


FIG. 3. (Color online) Equations of state for the three $c\text{-BC}_2\text{N}$ structures shown in Fig. 1: (a) calculated volume-pressure relations for HD1, HD2, and LD together with those of diamond ($c\text{-C}$) and cubic BN for comparison; (b) the volume ratio V/V_0 , with V_0 being the corresponding volume at zero pressure, for the two high-density phases; and (c) the volume ratio V/V_0 for the low-density phase.

The calculated electronic density of states for each of the three structures shown in Fig. 1 indicates that each of them is a semiconductor. This is consistent with experimental observations;^{25,26,36} the crystals appear to be transparent or possess an energy gap.

To see the difference between HD1 and HD2 structures, we need to take a close look of the atomic arrangement in them. Even though the bonding characteristics in both are similar, with C–C, C–N, C–B, and B–N bonds, there are carbon and boron-nitride layers embedded in HD1 which are a half of the lattice constant apart. Then a (200) peak is expected to show up in the x-ray diffraction pattern of HD1, as was observed by Zhao *et al.*²⁵ and Komatsu *et al.*²³ The (200) peak was originally interpreted as a signature of a superstructure of carbon and BN layers within the crystal.²⁵ However, it is not a surprise that no (200) peak appears in the x-ray diffraction pattern of HD2 because of the absence of layers; this is consistent with the high-density phase of Utsumi *et al.*²⁴ This is why we believe that HD1 represents the high-density phase synthesized by Utsumi *et al.*,²⁴ while HD2 represents the high-density phase synthesized by Zhao *et al.*²⁵ Of course, the (200) peak is not expected for the low-density phase because of the lack of such a superstructure there; this is consistent with what was found by Solozhenko *et al.*²⁶

In summary, we have resolved a long-standing problem in identifying the proper structures for the $c\text{-BC}_2\text{N}$ phases. Among many attempts in searching for a proper description of the low-density $c\text{-BC}_2\text{N}$ phase, N–N bonds were introduced¹⁵ to tune the lattice constant and bulk modulus to meet the experimental values. Our calculations indicate that the absence of C–C bonds in the proposed structure for the low-density phase weakens the bonding strength significantly. This causes enlarged lattice constant and lowered bulk modulus in the phase. Here, we have provided an accurate description of structural and energetic properties of

c-BC₂N phases. Careful analysis of the calculated results also offers important insights into the mechanism of the structural stability and transformation if pressure is applied to these phases.

We thank M. Nicol, K. Umemoto, and R. Wentzcovitch for stimulating discussions and helpful comments. This work is supported in part by DOE under Cooperative Agreement No. DE-FG36-05GO85028.

*Electronic address: kimej@physics.unlv.edu

- ¹N. Dubrovinskaia, L. Dubrovinsky, W. Crichton, F. Langenhorst, and A. Richter, *Appl. Phys. Lett.* **87**, 083106 (2005); N. Dubrovinskaia, S. Dub, and L. Dubrovinsky, *Nano Lett.* **6**, 824 (2006).
- ²R. B. Kaner, J. J. Gilman, and S. H. Tolbert, *Science* **308**, 1268 (2005).
- ³F. R. Bundy and R. H. Wentorf, Jr., *J. Chem. Phys.* **38**, 1144 (1963).
- ⁴F. R. Bundy and J. S. Kasper, *J. Chem. Phys.* **46**, 3437 (1967); F. R. Bundy, *Physica A* **156**, 169 (1989).
- ⁵E. Rapoport, *Ann. Chim. (Paris)* **10**, 607 (1985).
- ⁶F. R. Corrigan and F. P. Bundy, *J. Chem. Phys.* **63**, 3812 (1975).
- ⁷S. Nakano and O. Fukunaga, *Diamond Relat. Mater.* **2**, 1409 (1993).
- ⁸V. L. Solozhenko, *High Press. Res.* **13**, 199 (1995).
- ⁹V. L. Solozhenko, *Diamond Relat. Mater.* **4**, 1 (1994).
- ¹⁰C. S. Yoo, J. Akella, H. Cynn, and M. Nicol, *Phys. Rev. B* **56**, 140 (1997).
- ¹¹V. L. Solozhenko, V. Z. Turkevich, and W. B. Holzapfel, *J. Phys. Chem. B* **103**, 2903 (1999).
- ¹²J. Furthmüller, J. Hafner, and G. Kresse, *Phys. Rev. B* **50**, 15606 (1994).
- ¹³K. Albe, *Phys. Rev. B* **55**, 6203 (1997).
- ¹⁴G. Kern, G. Kresse, and J. Hafner, *Phys. Rev. B* **59**, 8551 (1999).
- ¹⁵H. Sun, S.-H. Jhi, D. Roundy, M. L. Cohen, and S. G. Louie, *Phys. Rev. B* **64**, 094108 (2001).
- ¹⁶A. Janotti, S.-H. Wei, and D. J. Singh, *Phys. Rev. B* **64**, 174107 (2001).
- ¹⁷W. J. Yu, W. M. Lau, S. P. Chan, Z. F. Liu, and Q. Q. Zheng, *Phys. Rev. B* **67**, 014108 (2003).
- ¹⁸E. Kim and C. Chen, *Phys. Lett. A* **319**, 384 (2003).
- ¹⁹E. Kim and C. Chen, *Phys. Lett. A* **326**, 442 (2004).
- ²⁰F. P. Bundy, *J. Chem. Phys.* **38**, 631 (1963).
- ²¹A. R. Badzian, *Mater. Res. Bull.* **16**, 1385 (1981).
- ²²S. Nakano, M. Akaishi, T. Sasaki, and S. Yamaoka, *Chem. Mater.* **6**, 2246 (1994).
- ²³T. Komatsu, M. Nomura, Y. Kakudae, and S. Fujiwara, *J. Mater. Chem.* **6**, 1799 (1996).
- ²⁴W. Utsumi, S. Nakano, K. Kimoto, T. Okada, M. Isshiki, T. Taniguchi, K. Funakoshi, M. Akaishi, and O. Shimomura, *Proceedings of AIRAPT-18, Beijing, China, 2001* (unpublished), p. 186.
- ²⁵Y. Zhao, D. W. He, L. L. Daemen, T. D. Shen, R. B. Schwarz, Y. Zhu, D. L. Bish, J. Huang, J. Zhang, G. Shen, J. Qian, and T. W. Zerda, *J. Mater. Res.* **17**, 3139 (2002).
- ²⁶V. L. Solozhenko, D. Andrault, G. Fiquet, M. Mezouar, and D. C. Rubie, *Appl. Phys. Lett.* **78**, 1385 (2001).
- ²⁷P. Hohenberg and W. Kohn, *Phys. Rev.* **136**, B864 (1964); W. Kohn and L. Sham, *Phys. Rev.* **140**, A1133 (1965).
- ²⁸J. P. Perdew, K. Burke, and M. Ernzerhof, *Phys. Rev. Lett.* **77**, 3865 (1996).
- ²⁹N. Troullier and J. L. Martins, *Phys. Rev. B* **43**, 1993 (1991).
- ³⁰H. J. Monkhorst and J. D. Pack, *Phys. Rev. B* **13**, 5188 (1976).
- ³¹C. Kittel, *Introduction to Solid State Physics*, 8th ed. (Wiley, New York, 2004), p. 80.
- ³²M. T. Yin and M. L. Cohen, *Phys. Rev. B* **26**, 5668 (1982).
- ³³F. D. Murnaghan, *Proc. Natl. Acad. Sci. U.S.A.* **30**, 244 (1944).
- ³⁴R. Gaudoin and W. M. C. Foulkes, *Phys. Rev. B* **66**, 052104 (2002).
- ³⁵E. Kim *et al.* (unpublished).
- ³⁶P. V. Zinin, V. L. Solozhenko, A. J. Malkin, and L. C. Ming, *J. Mater. Sci.* **40**, 3009 (2005).